APL Materials

RESEARCH ARTICLE | APRIL 03 2023

Room-temperature electric field-induced out-of-plane ferroelectric polarization in strain-free freestanding 2D $SrTiO_3$ membranes

Zhang et al.

Yueying Zhang; Jiaming Li; Ke Yang; ... et. al

APL Mater 11, 041103 (2023)
https://doi.org/10.1063/5.0144758

Room-temperature electric field-induced out-of-plane ferroelectric polarization in strain-free freestanding 2D $SrTiO_3$ membranes

Cite as: APL Mater. 11, 041103 (2023); doi: 10.1063/5.0144758
Submitted: 31 January 2023 • Accepted: 14 March 2023 •
Published Online: 3 April 2023

Yueying Zhang,[1,2] Jiaming Li,[3] Ke Yang,[4] Fangyuan Zheng,[4] Yuqing Zhou,[3] Yuguo Zhang,[1,2] Yupeng Hui,[1,2] Yue-Qi Wang,[1,2] Jiang Zhu,[1,2] Jincheng Zhang,[1,2,5] Yue Hao,[1,2,5] Ming Yang,[4] Tao Li,[3,a)] Jiong Zhao,[4,a)] and Haijiao Harsan Ma[1,2,5,a)]

AFFILIATIONS

[1] Low Dimensional Quantum Physics & Device Group, School of Microelectronics, Xidian University, 2 South Taibai Road, Xi'an 710071, China

[2] State Key Discipline Laboratory of Wide Band Gap Semiconductor Technology, School of Microelectronics, Xidian University, 2 South Taibai Road, Xi'an 710071, China

[3] Department of Materials Science and Engineering, Center for Spintronics and Quantum Systems, State Key Laboratory for Mechanical Behavior of Materials, Xi'an Jiaotong University, Xi'an 710049, China

[4] Department of Applied Physics, The Hong Kong Polytechnic University, Hung Hom, Hong Kong, China

[5] Collaborative Innovation Center of Quantum Information of Shaanxi Province, Xidian University, Xi'an 710071, China

[a)] **Authors to whom correspondence should be addressed:** taoli66@mail.xjtu.edu.cn; jiong.zhao@polyu.edu.hk; and mahj07@xidian.edu.cn

ABSTRACT

$SrTiO_3$ (STO), a room-temperature paraelectric material in bulk form, has been a rich playground for emergent phenomena for decades. As an emerging material, great attention has been paid to freestanding 2D STO thin films. Recently, the room-temperature ferroelectricity has been unveiled in strained STO thin films; however, it remains an open question whether the strain-free freestanding 2D STO thin film is room-temperature ferroelectric or not. Here, we report the electric field-induced out-of-plane ferroelectric polarization in large-scale, freestanding, and strain-free 2D STO membranes at room temperature. High-resolution piezoresponse force microscopy measurements show that polarization in freestanding strain-free STO membranes can be switched by electric field and persist for an hour. The first-principles calculations suggest that the intrinsic defects such as oxygen vacancies could be linked to the observed spontaneous out-of-plane polarization in 2D STO membranes, which could be further enhanced by external electric field due to the induced symmetry breaking. Our work reports the unprecedented room-temperature ferroelectric polarization in strain-free freestanding 2D STO membranes, unlocking the great potential of freestanding 2D STO for the applications in novel electronic and logic-in-memory devices.

Compared with conventional perovskites, freestanding perovskite thin films exhibit fascinating many-particle phenomena due to their low dimensionality and enhanced Coulombic interactions. As a typical perovskite oxide, freestanding $SrTiO_3$ (STO) thin films with thickness varying from a few unit cells to hundreds of nm have been successfully fabricated, which show intriguing physical properties such as excitons.[1] Furthermore, STO thin films demonstrate the potential as the high-k dielectric as a screening layer to realize skyrmions in perovskite oxides bilayers[2] or to achieve high-efficiency and low power-cost transistors.[3,4] In addition to the conventional applications such as substrates and electric insulator,[5,6] it is highly desirable to explore novel functionalities of STO. The realization of ferroelectricity in STO thin film offers an additional degree of freedom for tuning material functionalities, which enables STO thin film a potential candidate for multi-functional semiconductor devices, next-generation

complementary metal–oxide–semiconductor (CMOS) circuits, and emergent logic-in-memory devices.

STO has a cubic structure at room temperature, and it becomes tetragonal at temperature below 105–110 K at which ferroelastic–antiferroelectric phase transition occurs.[7–9] Although it possesses large dielectric constant up to 24 000 at 4 K,[10] STO remains the so-called quantum paraelectric at low temperatures, in which the long-range polarization order is suppressed by quantum fluctuations.[11] Nevertheless, the strain-induced polar state and ferroelectricity have been demonstrated in STO both in heteroepitaxy films and the bulk form. In 2004, Haeni *et al.* observed room-temperature in-plane polarization in tensile-strained STO films but no polarization in compressive-strained films.[12] Later in 2010, Jang *et al.* demonstrated relaxor ferroelectricity at low temperature in STO films grown on different substrates, in which strain-free film consisting of polar nanoregions with short correlation lengths plays a critical role.[13] Recently, Xu *et al.* reported in-plane room temperature ferroelectricity in chemically exfoliated freestanding 2D STO under external tensile strain up to 2%.[14] However, device with strain modulation by external force is rather difficult to be integrated into CMOS technologies. Alternatively, defect modulation-induced ferroelectricity has also been reported in STO.

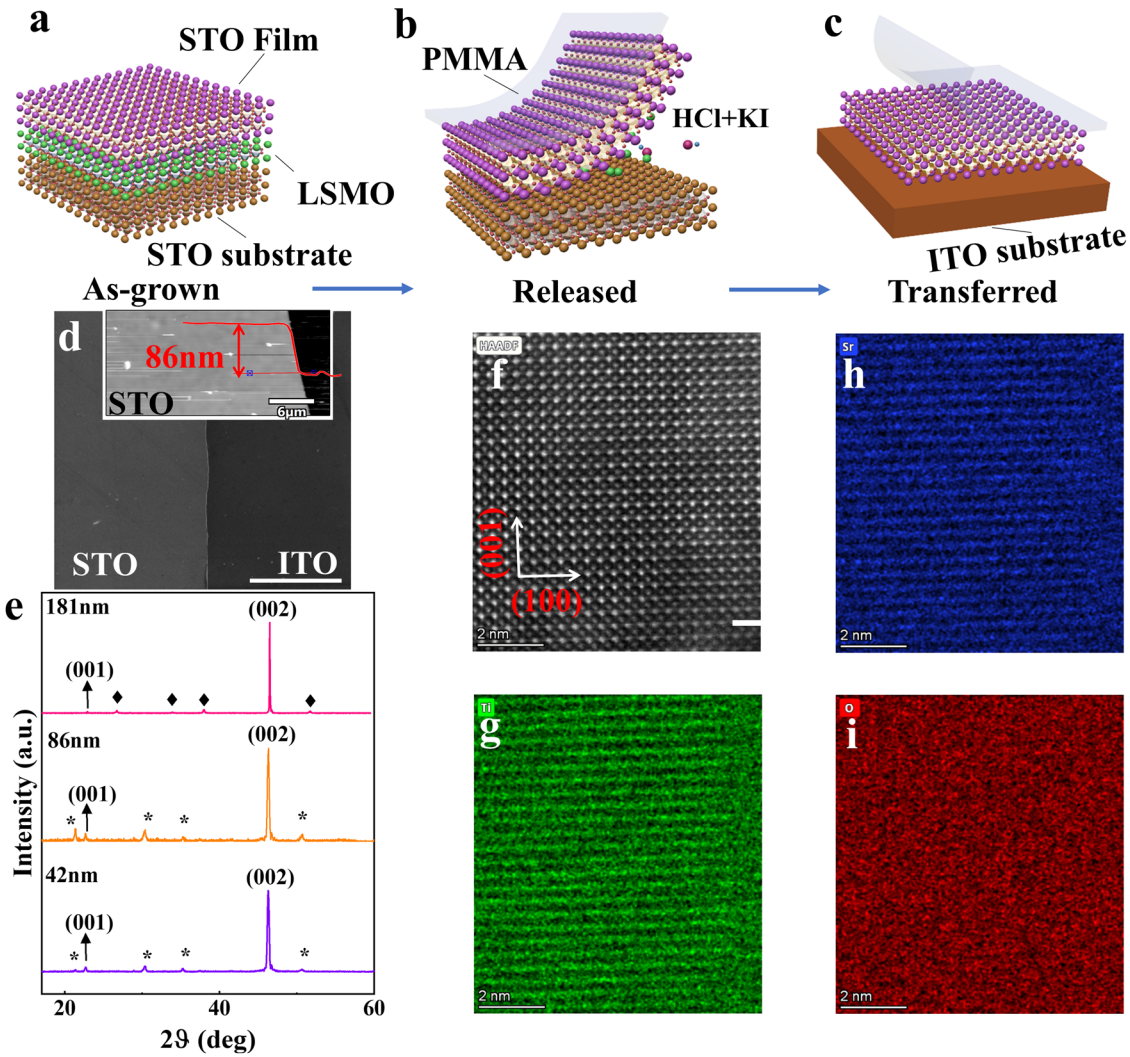

FIG. 1. Growth, transfer, and characterization of freestanding 2D $SrTiO_3$ (STO) membranes. (a), Schematic of a film with an LSMO buffer layer. (b) Sacrificial LSMO layer is dissolved in acid solution to release the top oxide films with the mechanical support of PMMA. (c) Freestanding STO membrane is transferred onto the desired substrate such as ITO glass. (d) SEM image of the freestanding STO membrane transferred onto the ITO substrate. The scale bar is 100 μm. Inset shows the AFM image of the STO film with a height profile showing a thickness of 86 nm. (e), XRD of STO membranes with different thicknesses. The (001) and (002) peaks of STO demonstrate high-quality membranes. The diamonds and stars indicate XRD peaks of FTO and ITO substrates, respectively. (f) Atomically resolved HAADF images of a cross-sectional freestanding STO membrane on ITO glass with scale bar of 2 nm (g)–(i) Elemental mapping of Ti (g), Sr. (h), and O (i), showing the high quality of freestanding STO film. The white scale bars are 2 nm in (g)–(i).

Room-temperature ferroelectric responses were reported in tetragonal STO grown under low oxygen pressure[15] and non-stoichiometric STO homoepitaxial films due to Ti/O deficient nanoregions.[16] In addition, metastable ferroelectricity was observed in bulk STO using optical excitation, which was associated with the light-induced thermal effect that leads to a phase transition into a metastable hidden ferroelectric phase.[17,18] Room-temperature ferroelectricity was also reported due to polar nanoregions in ultrathin $SrTiO_3$ films.[19]

In general, the ferroelectricity in STO has been realized by strain,[20] defect,[21] or phase engineering[22] in previous studies, which, however, come with additional difficulties to the potential applications. For example, phase transition due to doping requires precise control of material composition and structure, and it is difficult to integrate strain-induced ferroelectricity membranes with current CMOS technologies. Electric field modulation is a preferable method to control electronic devices comparing to strain and light.[23,24] Thus, purely electrically tuned room-temperature ferroelectricity in strain-free STO ultrathin film is appealing, especially in freestanding STO membranes with out-of-plane polarization, which can be transferred to random substrate regardless of lattice matching and can be used in wearable electronics. Furthermore, out-of-plane ferroelectrics can realize devices with high density due to its ability to scale down. However, strain-free freestanding 2D STO with out-of-plane ferroelectricity has not been reported so far.

Here, we report the electric field-induced ferroelectric polarization in 2D STO membranes by transferring the freestanding STO films onto conductive indium tin oxide (ITO) and fluorine-doped tin oxide (FTO) substrates. Using piezoresponse force microscopy and transmission electron microscopy, we show robust out-of-plane room-temperature polarization in 2D STO, corroborated by the characteristic feature of switchable 180° ferroelectric domains. We further reveal that the ferroelectric response is crystal orientation-dependent, and (001)-orientated STO membranes exhibit the most robust ferroelectricity. Our work demonstrates an effective way to realize ferroelectricity in 2D STO. It helps enhance ferroelectricity in freestanding STO membranes with out-of-plane polarization, enabling great promise for rich applications ranging from non-volatile memories to logic devices.

Homoexpitaxial STO thin films with a buffer layer of $La_{2/3}Sr_{1/3}MnO_3$ (LSMO) were grown on STO substrates, followed by chemical etching and transferring onto metallic substrates as the bottom electrodes [Figs. 1(a)–1(c)]. The details of the sample preparation are presented in the supplementary material. The morphology and crystallinity of the freestanding 2D STO membranes were characterized using scanning electron microscopy (SEM), atomic force microscopy (AFM), x-ray diffraction (XRD), and transmission electron microscopy (TEM). The SEM image of the STO membrane is shown in Fig. 1(d), and the inset shows the AFM image of the STO membrane on the ITO substrate with a height profile. The size of the freestanding STO membrane is in the range between 5 × 5 and 10 × 10 mm^2, and the typical thickness is in the range of 10–180 nm. The high quality of the freestanding STO membranes is further

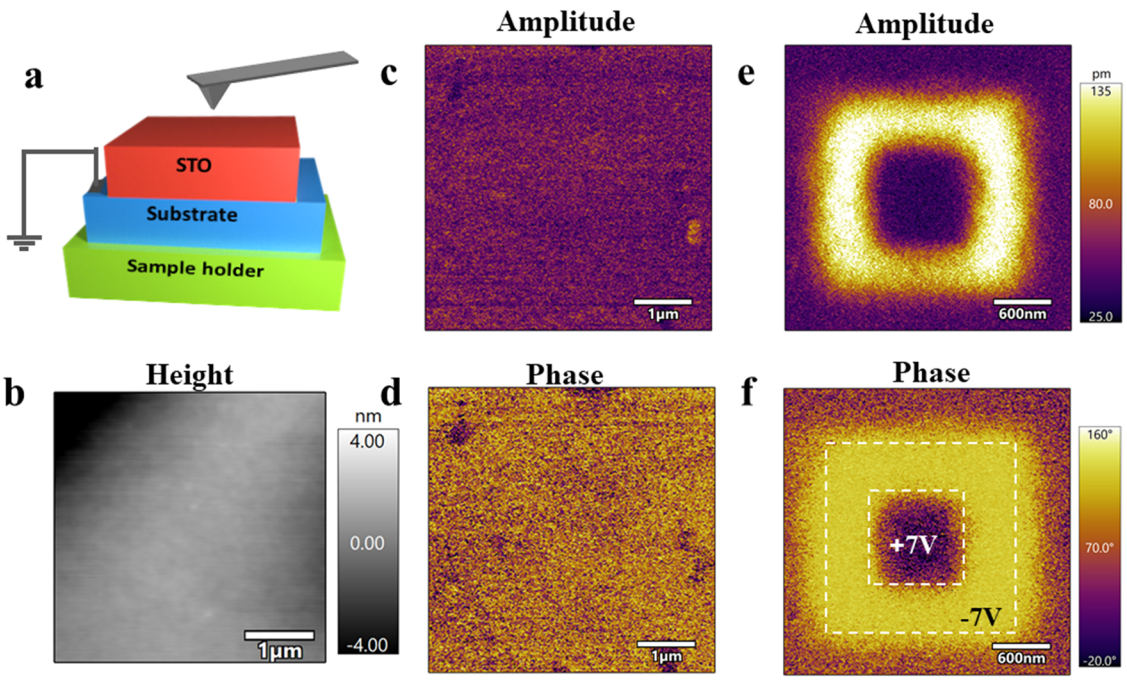

FIG. 2. Room-temperature out-of-plane polarization in (001)-oriented 2D STO membranes. (a) Schematic illustrating the measurement setup, wherein the STO membrane is transferred to a conductive substrate that is grounded. (b) Topographic image reveals crack-free smooth surface of STO membranes. PFM amplitude (c) and phase (d) signals of pristine STO membranes exhibit uniform weak piezoresponse. PFM amplitude (e) and phase (f) signals after applying poling voltage of −7 and 7 V through a conductive tip in the box-in-box patterned region. The image shows clear room-temperature ferroelectricity with notable 180° phase difference and corresponding amplitude contrast.

verified using the XRD measurement [Fig. 1(e)]. The (001)- and (002)- peak positions for STO (001) with different thicknesses are very close to that of bulk, indicating nearly strain-free 2D STO membranes [see Fig. S1 in the supplementary material for characterization and XRD data of (110)- and (111)- orientated STO membranes, Table T1 for the extracted lattice constant of freestanding 2D STO from XRD data, and Fig. S2 for SEM and optical images with larger size]. The diamonds and the stars in Fig. 1(e) denote the peak positions of FTO and ITO substrates, respectively. Figure 1(f) shows a cross-sectional high-angle annular dark-field (HAADF) image of STO (001) with atomic resolution, which shows good crystalline of the STO thin films. Elemental mapping spectroscopy images of Ti (g), Sr (h), and O (i) are shown in Figs. 1(g)–1(i). One can see clear boundaries among SrO and TiO_2 layers. All these characterization results suggest high quality of crystalline 2D STO membranes.

We performed a piezoresponse force microscopy (PFM) measurement on the 2D STO membranes with thicknesses varying from 19 to 292 nm using the experiment setup as illustrated in Fig. 2(a). The typical PFM responses of a 181 nm sample are shown in Fig. 2. The surface morphology of 2D STO is atomically smooth as demonstrated by atomic force microscopy (AFM) in Fig. 2(b). The pristine spontaneous ferroelectric response is presented in Figs. 2(c) and 2(d). The amplitude response, in general, is rather weak, but there are a few nanoregions showing stronger piezoresponse. It may exist intrinsic ferroelectric nanodomains in the pristine freestanding STO thin film. In addition, (111) and (110) oriented pristine STO membranes also show spontaneous polarization (Figs. S3-S6 in the supplementary material). To verify the out-of-plane ferroelectricity, +7 V and −7 V poling voltages are applied to the film surface through a conductive probe in a box-in-box pattern. Clearly, the ferroelectric domains are successfully switched to the upward and downward directions by −7 V and +7 V bias, respectively. However, no in-plane piezoresponse is observed in the samples.

The thickness-dependent ferroelectric polarization of STO films is further verified by PFM. PFM amplitude and the corresponding phase images of three samples electrically poled with −8 V and +8 V biases are shown in Figs. 3(a) and 3(b), respectively. These samples with different thicknesses demonstrate switchable polar regions. The domain wall between up- and down-oriented domains is clearly shown in the amplitude images. Switching spectroscopy PFM (SS-PFM) measurements were conducted to acquire the ferroelectric hysteresis loops. The phase and amplitude hysteresis loops observed from the 2D STO membranes are plotted in Figs. 3(c) and 3(d), respectively, which confirmed the presence of electric field switchable robust polarization. The thickness of STO does affect the polarization switching process. The thick STO (181 nm) shows a highly asymmetric amplitude loop, while the thin STO (42 nm) has rather symmetric amplitude loop. Usually, such asymmetry is due to the internal field or unbalanced screening conditions. In our case, the amplitude of thick STO relaxed faster than thin STO. The bulk properties start to dominate when STO becomes thicker. We also calculate the magnitude of the piezoresponse as shown in Fig. 3(e). The strength of the piezoresponse is almost linearly scales with a thickness for membranes below 181 nm, but it drops above that [see Fig. S3 in the supplementary material for PFM of thick STO (292 nm) and Fig. S4 for 19 nm STO]. It is possible that as the film thickness increases, the 2D STO membranes relax to the crystal structure of bulk, thus symmetry breaking induced by electric field or defects is reduced in thick films. We further analyzed coercive field E_c as a function of $1/d$ where d is the thickness [Fig. 3(f)]. The coercive field E_c varies in different scan loops for the same sample, leading to appearance of error bars. E_c scales with $1/d$. The inset shows the semilog plot of E_c vs $1/d$. Interestingly, there seems a critical thickness d_c, below and above which the scaling behaviors vary. We notice that the scaling of the coercive field over thickness extracted from switching spectroscopy PFM measurements (E_c scales with $1/d$) deviates from the common Kay–Dunn law[25] in which E_c scales with $d^{-2/3}$. The ferroelectric phase is destabilized at reduced thickness of perovskite-based materials, and the crystal lattice structure would relax to bulk in quite thick samples, e.g., ~300 nm, which could lead to a deviation from the Kay–Dunn law. A threshold field E_{th} of about 50 kV/cm can be extracted for thick membranes above 100 nm. For quasi-2D STO membranes with thickness around 10 nm, the coercive varies slowly and is close to saturate to ~3 MV/cm. Our previous work observed that a critical field of about 1.5 kV/cm is required for a field-induced ferroelectric order in single crystal tetragonal STO at 5 K.[26] The threshold field in the freestanding STO thin films at room temperature is about 30 times larger than that of the tetragonal single crystal STO at liquid helium temperature. Note that PFM responses are also observed in (111) and (110) freestanding 2D STOs, as shown in Figs. S5-S8 in the supplementary material, although it is strongest in (001) STO as shown in Figs. 2 and 3.

In addition, the polarization retention is another key parameter that needs to be evaluated for ferroelectric materials. In the case of the light-induced ferroelectricity of STO, a hidden metastable ferroelectric phase, which originates from the soft lattice vibrational mode induced by external excitation that is uncommon in phase diagrams, could be induced via mid-infrared or terahertz waves in bulk STO.[17,18] This metastable state exists up to a few hours and disappears at longer time scales. Here, we studied the time-dependent amplitude and phases of ferroelectric domains as shown in Fig. 4. As time evolves, the amplitude and phase contrast decay for 86-nm STO membranes [Figs. 4(a)–4(c)]. After 38 min from the electric poling, the amplitude and phase contrast become very weak. Similar behavior is observed from a 19-nm-thick STO membrane as shown in Figs. 4(d)–4(f). So that the electric field-enhanced polarization in the freestanding 2D STO thin film is also a metastable phenomenon. Figure S9 in the supplementary material shows similar behavior for the (111) STO membrane.

In order to understand the origin of the observed out-of-plane polarization, we conducted further density functional theory calculation. The results are shown in Fig. 5. Without an external electric field, the pristine 2D STO film shows an antiferroelectric ordering, where the local ionic distortions at the top and bottom surfaces are identical but with the opposite direction [see the atomic structure in Fig. 5(a)] due to the central inversion symmetry constrain. Therefore, there is no long-range spontaneous polarization in the pristine 2D STO film. In contrast, when an external electric field is applied, the lattice symmetry in 2D STO will be broken, leading to inequivalent lattice distortions that might contribute to long range and stable ferroelectric ordering, as shown in Fig. 5(b). The out-of-plane ferroelectric polarization can be further seen from the calculated electrostatic potential. As Fig. 5(c) shows, a net electrostatic potential of 1.8 eV is crossing the 2D STO structure when 0.5 V/Å electric field is applied, while for the pristine 2D STO

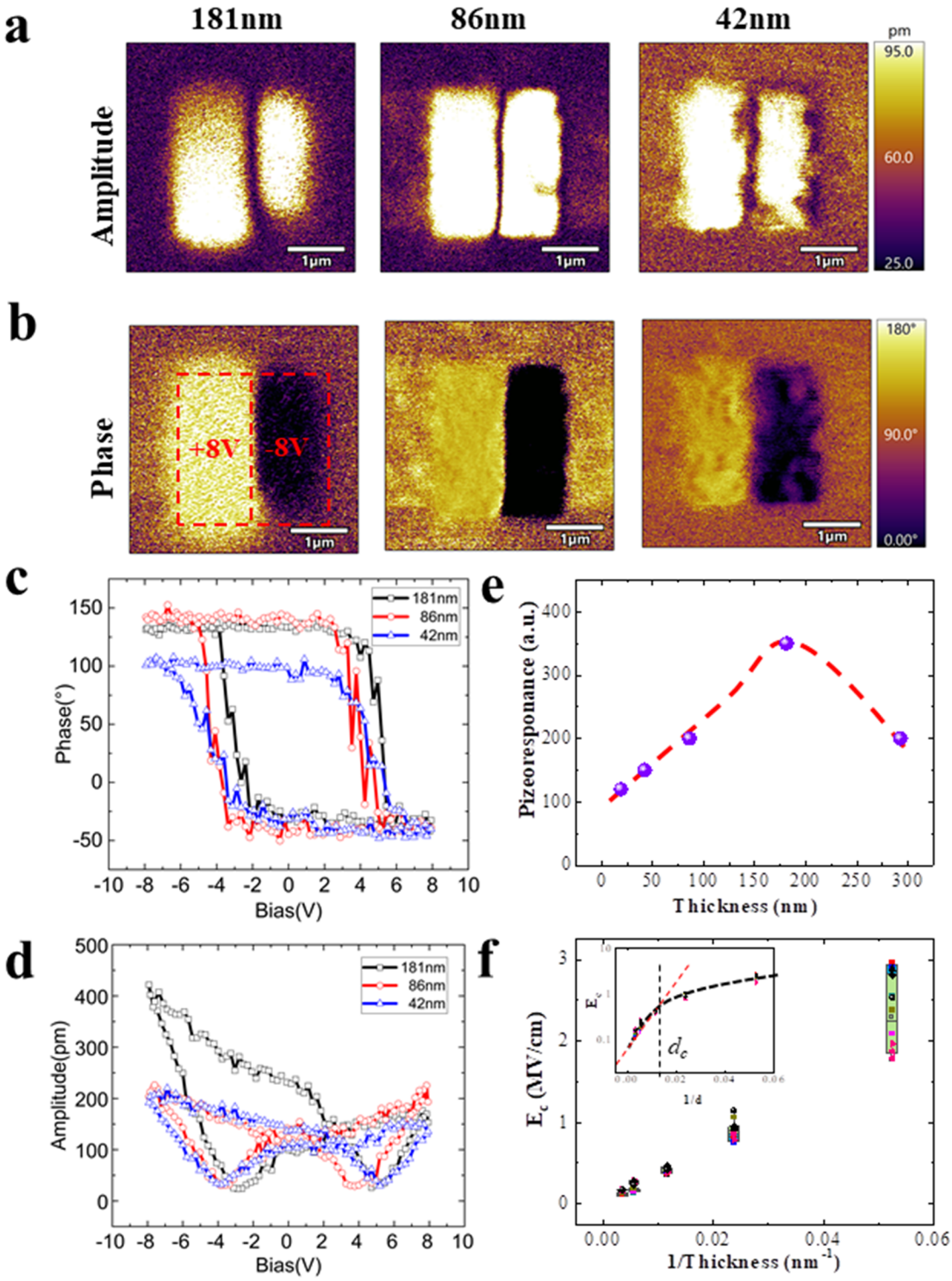

FIG. 3. Out-of-plane polarization switching and PFM hysteresis loops of strain-free freestanding STO membranes with different thicknesses. PFM amplitude (a) and phase (b) contrasts with switchable out-of-plane polarizations after applying positive +8 V (left) and negative −8 V (right) tip biases to the 2 × 2 μm^2 regions for three samples with different thicknesses. Phase (c) and amplitude (d) signal of remanent hysteresis loops. (e) Extracted PFM amplitude at −8 V as a function of thickness. The red line is a guideline showing electric field-induced polarization is almost linear to the thickness for films thickness below 200 nm. (f) Coercive field E_c as a function of 1/d where d is the thickness. Inset shows the semilog plot of E_c vs 1/d. The dark vertical dotted line indicates a critical thickness d_c.

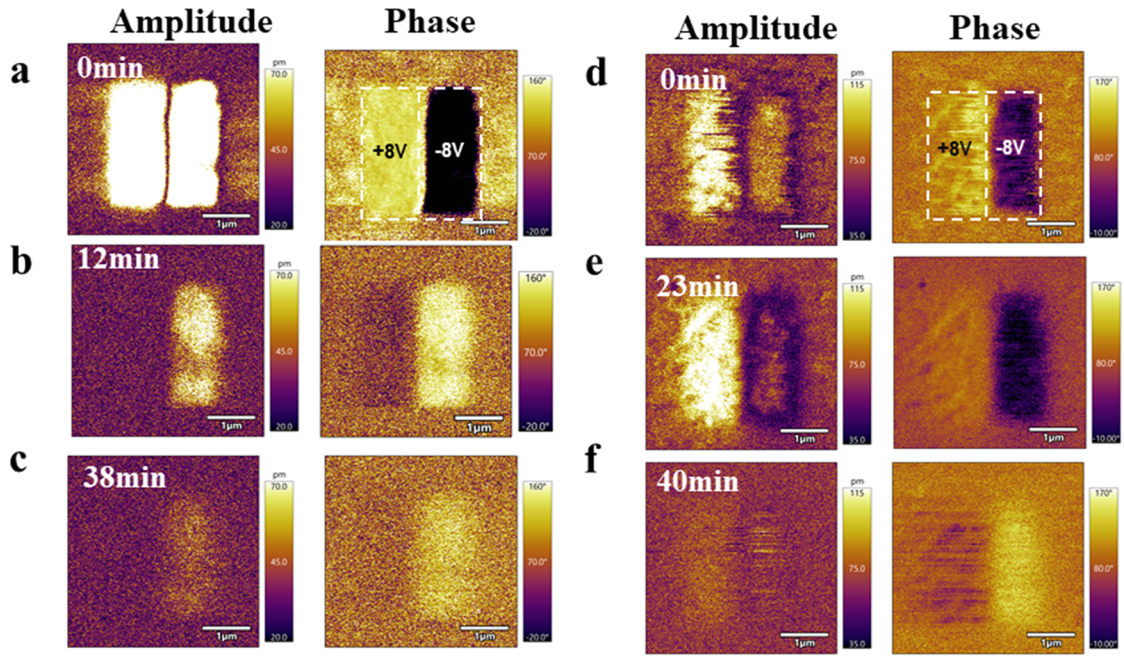

FIG. 4. Relaxation of electric field-induced ferroelectric polarization in freestanding 2D STO membranes. PFM amplitude and phase images with switchable out-of-plane polarizations measured immediately (a), 12 min (b) and 38 min (c) after applying +8 V and −8 V poling voltage on a STO membrane of 86 nm thick. PFM amplitude and phase images with out-of-plane polarizations measured immediately (d), 23 min (e) and 40 min (f) after applying a positive +8 V and negative −8 V tip bias for 19 nm STO membrane.

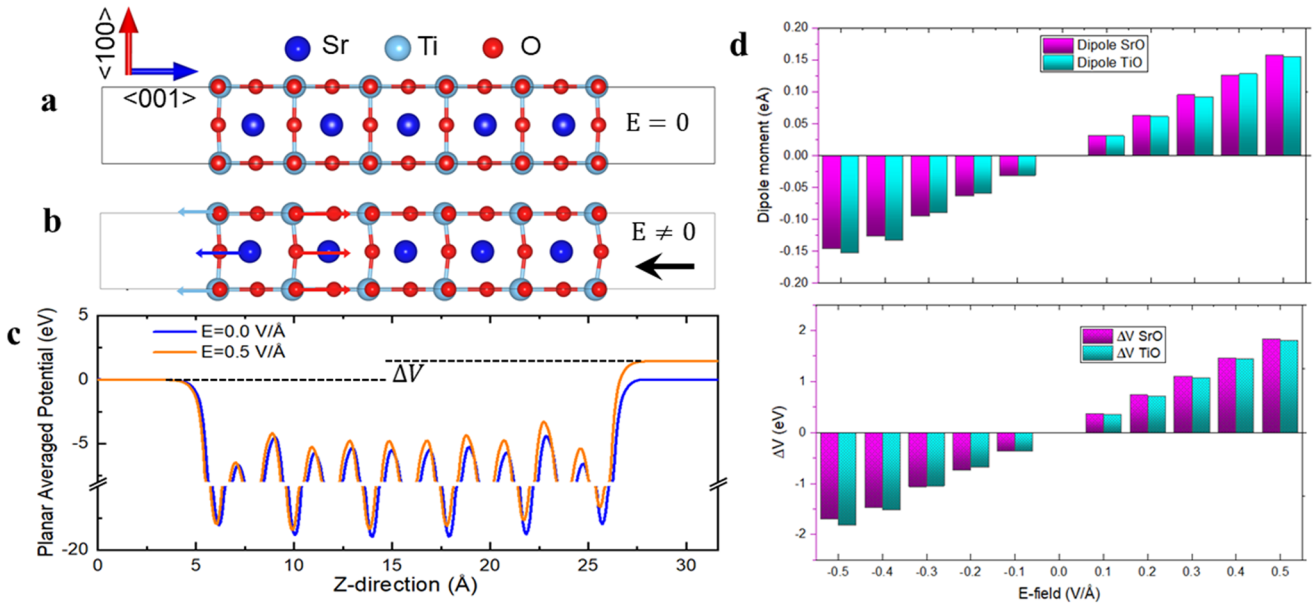

FIG. 5. Density functional theory (DFT) calculations. (a) and (b) Crystal structure of 2D STO without electric field (a) and with electric field (b). (c) Calculated averaged planar potential for (a) (blue line) and (b) (yellow line). (d) Calculated dipole moment and averaged planar potential in the STO 2D film under different electric fields.

without the electric field, there is no net electrostatic potential. This is consistent with the previous study which shows that the electric field can break the lattice symmetry of few-layer SnS and results in the ferroelectricity.[27] In Figs. 5(c) and 5(d), we can see that the dipole moment and the induced electrostatic potential in the 2D STO increase with the applied electric field, providing further evidence of the electric field-included ferroelectricity in 2D STO. Note that local polarization could be present by the intrinsic defects such as oxygen vacancies (Fig. S10 in the supplementary material), which could be connected to the observed electric field-induced polarization and ferroelectricity. The electric field has the effect to stabilize and enhance the out-of-plane ferroelectric polarization in freestanding STO membranes.

To conclude, room-temperature out-of-plane ferroelectricity and piezoelectricity were achieved in large-scale strain-free freestanding 2D STO membranes. The high-resolution PFM measurements show that switchable polarization could be induced by electric field and persist for about an hour. The typical coercive field to switch the polarization is about 1 MV/cm. The out-of-plane ferroelectric polarization in the 2D STO membranes can be stabilized and enhanced under electric field. The first-principles calculations suggest that the electric field breaks the lattice symmetry, leading to the out-of-plane ferroelectric polarization in the freestanding 2D STO membranes. This work proposed a method for modulating the functionality of a complex perovskite oxide.

The supplementary material includes details of experimental methods and theoretical calculation including sample preparation, density functional theory (DFT) calculations, piezoresponse force microscopy (PFM) measurements, transmission electron microscopy (TEM) characterization, and supporting data.

This work was supported by the National Key Research and Development Program of China (Grant Nos. 2021YFA0715600, 2021YFA1202200, and 2022YFB3605600). We thank the National Science Foundation (NSF) of China, Grant No. 61904140, for the financial support. M.Y. acknowledges the funding support from The Hong Kong Polytechnic University (Project Nos. 1-BE47, ZE0C, ZE2F, and ZE2X). H.H.M. acknowledges Ping Yang for useful discussions. M. Y. acknowledges the Centre for Advanced 2D Materials, the Centre of Information Technology at the National University of Singapore, and the National Supercomputing Center Singapore for providing computing resources. The work is supported by "the Fundamental Research Funds for the Central Universities" (Project No. QTZX23078).

AUTHOR DECLARATIONS

Conflict of Interest

The authors have no conflicts to disclose.

Author Contributions

Y.Z., J.L., K.Y., and F.Z. contributed equally to this work.

Yueying Zhang: Data curation (equal); Investigation (equal); Resources (equal); Visualization (equal); Writing – original draft (supporting); Writing – review & editing (equal). **Jiaming Li**: Data curation (equal); Investigation (equal); Validation (supporting); Visualization (supporting). **Ke Yang**: Formal analysis (equal); Resources (equal); Writing – original draft (supporting). **Fangyuan Zheng**: Data curation (equal); Formal analysis (equal); Visualization (supporting). **Yuqing Zhou**: Investigation (equal); Validation (supporting). **Yuguo Zhang**: Visualization (supporting). **Yupeng Hui**: Investigation (supporting). **Yue-Qi Wang**: Investigation (supporting). **Jiang Zhu**: Conceptualization (supporting). **Jincheng Zhang**: Conceptualization (supporting); Resources (supporting). **Yue Hao**: Conceptualization (supporting); Resources (supporting). **Ming Yang**: Resources (equal); Supervision (equal); Writing – review & editing (equal). **Tao Li**: Conceptualization (supporting); Resources (equal); Supervision (equal); Writing – review & editing (equal). **Jiong Zhao**: Resources (equal); Supervision (equal). **Haijiao Harsan Ma**: Conceptualization (equal); Resources (equal); Writing – original draft (equal); Writing – review & editing (equal).

DATA AVAILABILITY

The data that support the findings of this study are available within the article and its supplementary material.

REFERENCES

[1] Y. Zhang *et al.*, "Emergent midgap excitons in large-size freestanding 2D strongly correlated perovskite oxide films," Adv. Opt. Mater. **9**, 2100025 (2021).
[2] L. Han *et al.*, "High-density switchable skyrmion-like polar nanodomains integrated on silicon," Nature **603**, 63–67 (2022).
[3] A. J. Yang *et al.*, "Van der Waals integration of high-κ perovskite oxides and two-dimensional semiconductors," Nat. Electron. **5**, 233–240 (2022).
[4] J.-K. Huang *et al.*, "High-κ perovskite membranes as insulators for two-dimensional transistors," Nature **605**, 262–267 (2022).
[5] K. A. Parendo, K. H. S. B. Tan, A. Bhattacharya, M. Eblen-Zayas, N. E. Staley, and A. M. Goldman, "Electrostatic tuning of the superconductor-insulator transition in two dimensions," Phys. Rev. Lett. **94**, 197004 (2005).
[6] C.-Z. Chang *et al.*, "Experimental observation of the quantum anomalous Hall effect in a magnetic topological insulator," Science **340**, 167–171 (2013).
[7] L. Rimai and G. A. Demars, "Electron paramagnetic resonance of trivalent gadolinium ions in strontium and barium titanates," Phys. Rev. **127**, 702–710 (1962).
[8] F. W. Lytle, "X-ray diffractometry of low-temperature phase transformations in strontium titanate," J. Appl. Phys. **35**, 2212–2215 (1964).
[9] V. V. Lemanov, "Improper ferroelastic $SrTiO_3$ and what we know today about its properties," Ferroelectrics **265**, 1–21 (2002).
[10] K. A. Müller and H. Burkard, "$SrTiO_3$: An intrinsic quantum paraelectric below 4 K," Phys. Rev. B **19**, 3593–3602 (1979).
[11] M. Takesada, M. Itoh, and T. Yagi, "Perfect softening of the ferroelectric mode in the isotope-exchanged strontium titanate of $SrTi^{18}O_3$ studied by light scattering," Phys. Rev. Lett. **96**, 227602 (2006).
[12] J. H. Haeni *et al.*, "Room-temperature ferroelectricity in strained $SrTiO_3$," Nature **430**, 758–761 (2004).
[13] H. W. Jang *et al.*, "Ferroelectricity in strain-free $SrTiO_3$ thin films," Phys. Rev. Lett. **104**, 197601 (2010).
[14] R. Xu *et al.*, "Strain-induced room-temperature ferroelectricity in $SrTiO_3$ membranes," Nat. Commun. **11**, 3141 (2020).
[15] Y. S. Kim *et al.*, "Observation of room-temperature ferroelectricity in tetragonal strontium titanate thin films on $SrTiO_3$ (001) substrates," Appl. Phys. Lett. **91**, 042908 (2007).
[16] T. Li *et al.*, "Strong room-temperature ferroelectricity in strained $SrTiO_3$ homoepitaxial film," Adv. Mater. **33**, 2008316 (2021).

[17]T. F. Nova, A. S. Disa, M. Fechner, and A. Cavalleri, "Metastable ferroelectricity in optically strained $SrTiO_3$," Science **364**, 1075–1079 (2019).
[18]X. Li *et al.*, "Terahertz field–induced ferroelectricity in quantum paraelectric $SrTiO_3$," Science **364**, 1079–1082 (2019).
[19]D. Lee *et al.*, "Emergence of room-temperature ferroelectricity at reduced dimensions," Science **349**, 1314–1317 (2015).
[20]A. Vasudevarao *et al.*, "Multiferroic domain dynamics in strained strontium titanate," Phys. Rev. Lett. **97**, 257602 (2006).
[21]Y. S. Kim *et al.*, "Defect-related room-temperature ferroelectricity in tensile-strained $SrTiO_3$ thin films on $GdScO_3$ (110) substrates," Appl. Phys. Lett. **97**, 242907 (2010).
[22]T. Mitsui and W. B. Westphal, "Dielectric and X-ray studies of $Ca_xBa_{1-x}TiO_3$ and $Ca_xSr_{1-x}TiO_3$," Phys. Rev. **124**, 1354–1359 (1961).
[23]M. Liu *et al.*, "Giant electric field tuning of magnetic properties in multiferroic ferrite/ferroelectric heterostructures," Adv. Funct. Mater. **19**, 1826–1831 (2009).
[24]H. J. H. Ma and J. F. Scott, "Non-ohmic variable-range hopping and resistive switching in $SrTiO_3$ domain walls," Phys. Rev. Lett. **124**, 146601 (2020).
[25]N. Tasneem *et al.*, "A Janovec–Kay–Dunn-like behavior at thickness scaling in ultra-thin antiferroelectric ZrO_2 films," Adv. Electron. Mater **7**, 2100485 (2021).
[26]H. J. H. Ma *et al.*, "Local electrical imaging of tetragonal domains and field-induced ferroelectric twin walls in conducting $SrTiO_3$," Phys. Rev. Lett. **116**, 257601 (2016).
[27]Y. Bao *et al.*, "Gate-tunable in-plane ferroelectricity in few-layer SnS," Nano Lett. **19**, 5109–5117 (2019).